Reversible, linear-sweep voltammetry of a soluble redox couple: effect of initial concentrations

ARTICLE *in* ANALYTICAL CHEMISTRY · APRIL 1990

Impact Factor: 5.64 · DOI: 10.1021/ac00207a022

2 AUTHORS, INCLUDING:

John W Weidner
University of South Carolina
160 PUBLICATIONS **3,014** CITATIONS

(29) Harris, Jr., W. C.; Chandra, S.; Morrison, G. H. *Anal. Chem.* **1983**, *55*, 1959.
(30) Tamaki, S.; Sichtermann, W. K.; Benninghoven; A.; *Jpn. J. Appl. Phys.* **1984**, *2*, 544.
(31) Hearn, M. J.; Briggs, D.; Yoon, S. C.; Ratner; B. D. *SIA, Surf. Interface Anal.* **1987**, *10*, 524.
(32) Hues, S. M.; Colton, R. J.; Mowery, R. L.; McGrath, K. J.; Wyatt, J. R. *Appl. Surf. Sci.* **1989**, *35*, 507.
(33) Clark, M. B., Jr.; Gardella, J. A., Jr.; Schultz, T. M.; Salvati, L., Jr.; Patil, D. G. *Anal. Chem.*, in press.
(34) Clark, M. B., Jr. Ph.D. Thesis, State University of New York at Buffalo, 1989.
(35) Kurtz, S. K.; Schultz, T. M.; Wolfram, L. J. *Crystal Structure of Melanin Precursors*. Presented at the First Pan American Society for Pigment Cell Research Meeting; University of Minneapolis Medical School; Minneapolis, MN, June 1988.
(36) Roychowdhury, P.; Black, B. S. *Acta Crystallogr.* **1975**, *B31*, 1559.
(37) Busch, K. L.; Bih, H. H.; Ya-Xiang, X.; Cooks, R. G. *Anal. Chem.* **1983**, *55*, 1157.
(38) Lui, L. K.; Busch, K. L.; Cooks, R. G. *Anal. Chem.* **1981**, *53*, 109.
(39) Cooks, R. G.; Busch, K. L. *Int. J. Mass Spectrom. Ion. Phys.* **1983**, *53*, 111.
(40) Cornelio, P. A.; Clark, M. B., Jr.; Gardella, J. A., Jr. In *Secondary Ion Mass Spectrometry (SIMS) VII*, Benninghoven, A., Ed.; Springer Verlag, in press.

RECEIVED for review August 7, 1989. Accepted January 16, 1990. The authors thank the Lawrence M. Gelb Research Foundation and the National Science Foundation, Division of Materials Research (Polymer Program) Grant Number 8720650 for the financial support of this study.

CORRESPONDENCE

Reversible, Linear-Sweep Voltammetry of a Soluble Redox Couple: Effect of Initial Concentrations

Sir: Classical theoretical formulas are available to predict the peak current and potential at a planar electrode during linear-sweep voltammetry (LSV) for the reversible (Nernstian) reaction

$$O + ne^- \rightleftharpoons R \quad (1)$$

where O and R are soluble oxidized and reduced species, respectively, and n is the number of electrons transferred (*1*, *2*). Matsuda and Ayabe (*1*) and Nicholson and Shain (*2*) showed that if the reduced species is present initially in negligible amounts and the voltage is swept in the negative direction, the cathodic peak current is proportional to the absolute value of the sweep rate to the one-half power and the corresponding peak potential is sweep-rate independent. Matsuda and Ayabe (*1*) also demonstrated that if the sweep begins at the equilibrium potential, E_{eq}, the dimensionless peak current and potential depend only upon the product of two dimensionless ratios, $\gamma\theta^*$: the ratio of the square root of the diffusion coefficients of O and R, $\gamma \equiv (D_O/D_R)^{1/2}$, and the initial concentration ratio of O and R in the bulk electrolyte, $\theta^* \equiv (C_O^*/C_R^*)$. Matsuda and Ayabe (*1*) presented calculations for the case where $\gamma\theta^* \rightarrow \infty$. Left numerically unexamined was the influence of R when its concentration is not negligibly small. Farsang et al. (*3*), using the same formula as derived by Matsuda and Ayabe (*1*), examined the influence of $\gamma\theta^*$ on the peak values over the narrow range of $0.22 \leq \gamma\theta^* \leq 5.5$ and found a shift in the potential to more negative values and an increase in the dimensionless peak current as $\gamma\theta^*$ decreased.

Nicholson and Shain (*2*) considered the case of starting the sweep at a nonequilibrium potential, E_i, in the limit of the reduced species concentration equal to zero ($\theta^* = \infty$). They obtained a current–potential relationship which is a function of an analogous dimensionless grouping, $\gamma\theta$, where γ is the same as defined above, and θ is the concentration ratio at the *electrode surface* given by the Nernst equation immediately *after* E_i is applied. This nonequilibrium initial condition gives rise to a Cottrell current in the early portion of the sweep, which they showed does not significantly affect the peak current or potential as long as $\gamma\theta > 650$. This corresponds to starting the sweep at a potential that is at least $200/n$ mV (T = 25 °C) positive of the peak potential.

In what follows, the Matsuda and Ayabe (*1*) equation is applied to calculate the peak potential and current over the range of $\gamma\theta^*$ from zero to infinity. Also presented is an explicit heretofore unrecognized formula for the peak values in the limit of $\gamma\theta^* \rightarrow 0$. The peak values at the two limiting behaviors are used to deduce and develop an easy-to-apply empirical relationship which correlates the results as a function of $\gamma\theta^*$ over the entire range. The calculations are confirmed by experimental measurements. The effect of mistakingly applying the Nicholson and Shain (*2*) formula for regions of $\gamma\theta^*$ below its range of validity is also quantified.

PEAK CURRENT AND POTENTIAL CALCULATIONS

Matsuda and Ayabe (*1*) solved the one-dimensional transient diffusion equation for both soluble redox species and obtained the time-dependent surface concentrations for O and R in terms of the reaction current. Starting the sweep at the equilibrium potential, θ^* is related to E_{eq} by

$$\theta^* = \exp\left[\left(\frac{nF}{RT}\right)(E_{eq} - E^{\circ\prime})\right] \quad (2)$$

where $E^{\circ\prime}$ is the formal potential. For the case of reversible kinetics, substituting eq 2, the surface concentrations and the sweep rate, v, into the Nernst equation results in the integral equation for the current

$$\int_0^{at} \frac{\chi(z)\,dz}{(at - z)^{1/2}} = \frac{1 - \exp(-at)}{1 + \gamma\theta^* \exp(-at)} \equiv L(at) \quad (3)$$

where t is time, $a \equiv (nF/RT)v$ which is positive for a cathodic sweep, and $\chi(at)$ is the dimensionless current defined as

$$\pi^{1/2}\chi(at) \equiv \frac{i(at)}{nFAC_O^*(D_O a)^{1/2}} \quad (4)$$

where F is Faraday's constant, A is the electrode area, and $i(at)$ is the time-dependent reaction current that is positive for a cathodic reaction. The product (at) is the displacement of the dimensionless potential from the starting potential.

Equation 3 differs from the analogous formula given by Nicholson and Shain (eq 22 of ref 2) in that by their as-

0003-2700/90/0362-0875$02.50/0

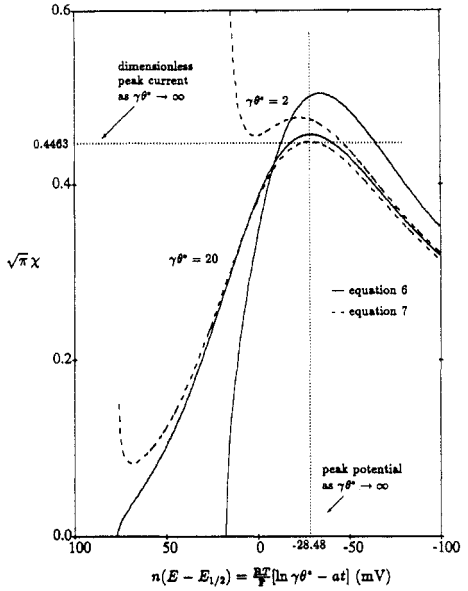

Figure 1. Predicted linear-sweep voltammograms from a planar electrode. The solid lines are the voltammograms generated from eq 6. The dashed lines are voltammograms generated from eq 7 with θ replaced by θ^*. The potentials, in mV, are for T = 298 K.

sumption of C_R^* is equal to zero, the numerator of $L(at)$ is equal to one, and θ^* is replaced by θ where θ is given by

$$\theta = \exp\left[\left(\frac{nF}{RT}\right)(E_i - E^{\circ\prime})\right] \tag{5}$$

Equation 3 is an Abel integral equation (5) for $\chi(at)$ with the solution

$$\pi^{1/2}\chi(at) = \frac{(1 + 1/\gamma\theta^*)}{4\pi^{1/2}} \int_0^{at} \frac{dz}{(at - z)^{1/2} \cosh^2[(\ln \gamma\theta^* - z)/2]} \tag{6}$$

The analogous current–potential relationship derived by Nicholson and Shain (eq 33 of ref 2) from the solution of eq 3 with a unity numerator for $L(at)$ and θ replaced by θ^* is

$$\pi^{1/2}\chi(at) = \frac{1}{[\pi(at)]^{1/2}(1 + \gamma\theta)} + \frac{1}{4\pi^{1/2}} \int_0^{at} \frac{dz}{(at - z)^{1/2} \cosh^2[(\ln \gamma\theta - z)/2]} \tag{7}$$

(For the calculations presented here, the integrals in eq 6 and 7 were numerically evaluated by using the IMSL (6) quadrature subroutine DQDAGS which accommodates integrands having end-point singularities.)

Although eq 6 as $\gamma\theta^* \to \infty$ is identical with the $\gamma\theta \to \infty$ limit of eq 7, θ^* and θ are not interchangeable. The leading term in eq 7 is a result of assuming the initial concentration of the reduced species is zero and predicts a Cottrell current upon application of E_i at the start of the sweep. This term can be significant when $\gamma\theta$ is not large. To illustrate this point, the effect on the voltammogram of erroneously replacing θ with θ^* in eq 7 is shown in Figure 1 with the potentials plotted relative to the half-wave potential, $E_{1/2} \equiv E^{\circ\prime} + (RT/nF) \ln \gamma$ (2). At $\gamma\theta^* = 20$, the dimensionless peak current and potential predicted from eq 6 both differ from those found by using eq 7 (with θ set equal to θ^*) by 2%, and at $\gamma\theta^* = 2$, the percentage difference is 6% and 33%, respectively.

The dimensionless peak current and potential may be determined as a function of $\gamma\theta^*$ by calculating the voltammogram using eq 6 to locate graphically the peak position.

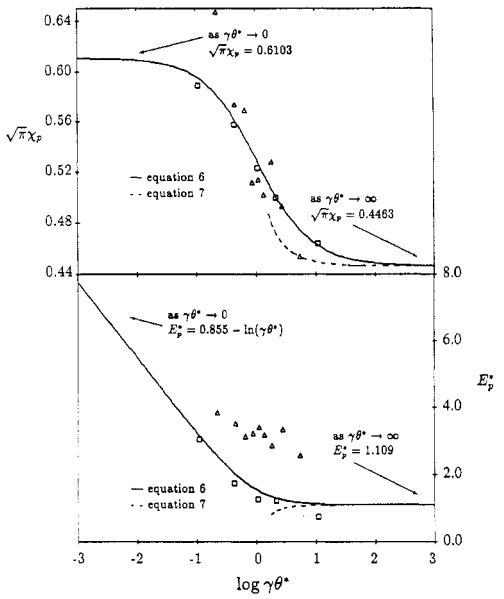

Figure 2. Dimensionless peak currents and potentials for linear-sweep voltammetry on a planar electrode as a function of $\gamma\theta^*$. The solid lines result from the use of eq 6, and the dashed lines result from the use of eq 7 with θ replaced by θ^*. For $\gamma\theta^* \leq 1.60$, eq 7 cannot predict peak values. The symbols are the peak values which were obtained experimentally using the $Fe(CN)_6^{4-}/Fe(CN)_6^{3-}$ redox couple. Key: □, present results; △, Tomcsanyi et al. (4) data.

However, a more convenient analytical procedure was derived by differentiating eq 6 with respect to (at) and setting the result equal to zero. The potential that satisfies the resulting expression is the peak potential which, when substituted into eq 6, specifies the peak current. Newton's method was used to solve the resulting nonlinear equation for the peak potential generated from this procedure. The same technique was applied to eq 7 (with θ replaced by θ^*) and the resulting dimensionless peak currents and potentials from the two predictions are compared in Figure 2 as a function of $\gamma\theta^*$. The dimensionless peak potential, E_p^*, is defined as

$$E_p^* \equiv [(at)_p - \ln \gamma\theta^*] \tag{8}$$

where $(at)_p$ is the dimensionless peak potential relative to the equilibrium potential.

Nicholson and Shain (2) report their results at $\gamma\theta$ = 650, and Matsuda and Ayabe report theirs at $\gamma\theta^*$ = 165 000, and from Figure 2 we see that θ and θ^* are interchangeable at these values; that is, no difference is found in the predicted peak values regardless whether eq 6 or 7 is used. Replacing θ^* with θ at smaller values of θ^*, however, will lead to differing results. Further, for values of $\gamma\theta^* \leq 1.60$, eq 7 does not predict a peak current because the Cottrell current dominates the transient response.

The dimensionless peak values ($\pi^{1/2}\chi_p$ = 0.4463 and E_p^* = 1.109) given by Matsuda and Ayabe (1) and Nicholson and Shain (2) are the limiting values as $\gamma\theta^* \to \infty$. Limiting values for the dimensionless peak current and potential can also be obtained for $\gamma\theta^* \to 0$ by taking the limit of eq 6 as $\gamma\theta^*$ approaches zero which, after some mathematical manipulation, results in

$$\pi^{1/2}\chi(at)|_{\gamma\theta^* \to 0} = \frac{1}{\pi^{1/2}} \int_0^{at} \frac{\exp(-z)}{(at - z)^{1/2}} dz \tag{9}$$

Following the analogous calculus procedure applied to eq 6 to calculate the peak potential, Newton's method was applied to determine numerically $(at)_p$ = 0.855 in the limit of $\gamma\theta^* \to 0$. The corresponding dimensionless peak current found from eq 9 is 0.6103.

EMPIRICAL CORRELATIONS

The following one parameter empirical relationship, motivated by the asymptotic trends seen in Figure 2, was fit to the theoretically predicted dimensionless peak currents from eq 6

$$\pi^{1/2}\chi_p(\gamma\theta^*) = \pi^{1/2}\chi_p(0) - [\pi^{1/2}\chi_p(0) - \pi^{1/2}\chi_p(\infty)]\left[\frac{\gamma\theta^*}{m + \gamma\theta^*}\right] \quad (10)$$

where $\pi^{1/2}\chi_p(0)$ and $\pi^{1/2}\chi_p(\infty)$ are the known dimensionless peak currents at the limits $\gamma\theta^* \to 0$ and $\gamma\theta^* \to \infty$, respectively, and m is an empirical parameter which was found by least-squares fit of eq 10 to the data in Figure 2. The resulting correlation is

$$\pi^{1/2}\chi_p(\gamma\theta^*) = 0.6103 - 0.164\left[\frac{\gamma\theta^*}{1.08 + \gamma\theta^*}\right] \quad (11)$$

The following one parameter empirical relationship, also motivated by the asymptotic trends seen in Figure 2, was fit to the theoretically predicted peak potentials from eq 6

$$E_p^*(\gamma\theta^*) = \ln\{[\exp E_p^*(0)]^m + [\exp E_p^*(\infty)]^m\}^{1/m} \quad (12)$$

where $E_p^*(0)$ and $E_p^*(\infty)$ are the known dimensionless peak potentials at the limits $\gamma\theta^* \to 0$ and $\gamma\theta^* \to \infty$, respectively. The parameter m was found by least-squares fit to the data in Figure 2. The resulting correlation is

$$E_p^*(\gamma\theta^*) = \ln\left[\left(\frac{2.35}{\gamma\theta^*}\right)^{1.19} + 3.74\right]^{0.84} \quad (13)$$

For $0 < \gamma\theta^* < \infty$, eqs 11 and 13 deviate from the exact values by at most 0.1% and 1%, respectively, differences which are visually indistinguishable in Figure 2. The maximum 1% error resulting from eq 13 (which occurs in the vicinity of $\gamma\theta^* = 3$) translates to less than a 0.5 mV ($n = 1$ and $T = 298$ K) error which is experimentally insignificant.

EXPERIMENTAL RESULTS

Linear-sweep voltammetry was conducted by using the ferro/ferricyanide redox couple in 1.0 M KCl at five different concentration ratios. The concentration of the ferricyanide was maintained at 0.010 M, and five different ferrocyanide concentrations were used: 0.0010 M, 0.0050 M, 0.010 M, 0.025 M, and 0.10 M. Cottrell experiments were run in order to determine γ by taking the ratio of the product of $(it^{1/2})$ for oxidation-to-reduction experiments, and $\gamma = 1.09$ was obtained which agrees within 1% of that calculated by using the diffusion coefficients for O and R given by Adams (7). Therefore, the $\gamma\theta^*$ values for the five concentrations ratios are 10.9, 2.18, 1.09, 0.436, and 0.109. All experiments were performed in a single-compartment cell at room temperature with a 1.6 mm diameter Pt disk as the working electrode which was not perfectly flush with the surface, and Ag/AgCl as the reference electrode. Voltammograms were generated at nine different sweep rates ranging from 4 to 150 mV/s and were run in duplicate. The *dimensionless* peak current, $\pi^{1/2}\chi_p$, was obtained by plotting the *dimensional* peak current, i_p, versus the absolute value of the sweep rate to the one-half power, $|v|^{1/2}$. The slope, $di_p/d|v|^{1/2}$, resulting from linear regression of these data was used to calculate $\pi^{1/2}\chi_p$ since from eq 4

$$\pi^{1/2}\chi_p(\gamma\theta^*) = \frac{(RT)^{1/2}}{(nF)^{3/2}C_O^* A D_O^{1/2}}\frac{di_p}{d|v|^{1/2}} \quad (14)$$

The unknown product $AD_O^{1/2}$ was determined by performing a series of linear sweeps at which only the oxidized species was present ($\gamma\theta^* = \infty$) and solving eq 14 for $AD_O^{1/2}$ using $\pi^{1/2}\chi_p = 0.4463$. The product $AD_O^{1/2}$ calculated in this manner was then used in eq 14 at the lower values of $\gamma\theta^*$ to obtain $\pi^{1/2}\chi_p(\gamma\theta^*)$. The peak potential, $(at)_p$, which is independent of the sweep rate, was read directly from the voltammogram for each value of $\gamma\theta^*$, and eq 8 was used to calculate E_p^*.

The experimental dimensionless peak currents and potentials (open squares) are compared to the theoretical values in Figure 2. The experimentally determined peak currents deviate from those theoretically predicted by at most 1%. The measured peak potentials also closely agree with those predicted, except for $\theta^* = 10$ at which a 10-mV deviation occurs. Also included in Figure 2 are the experimental data reported by Tomcsanyi et al. (4) (open triangles) from LSV run on a Pt electrode in 1.0 M KCl using the ferro/ferricyanide redox couple. The scatter is larger in these data, but the trend in $\pi^{1/2}\chi_p(\gamma\theta^*)$ is evident. The peak potentials obtained by Tomcsanyi et al. (4) were reported only to the nearest 10 mV and are 30–40 mV higher than the theory predicts.

Registry No. $Fe(CN)_6^{4-}$, 13408-63-4; $Fe(CN)_6^{3-}$, 13408-62-3.

LITERATURE CITED

(1) Matsuda, Hiroaki; Ayabe, Yuzo *Z. Elektrochem.* **1955**, *59*, 494–503.
(2) Nicholson, Richard S.; Shain, Irving *Anal. Chem.* **1964**, *36*, 706–723.
(3) Farsang, Gyorgy; Rozsondai, Bela; Tomcsanyi, Laszlo *Magy. Kem. Foly.* **1970**, *76*, 233–236.
(4) Tomcsanyi, Laszlo; Farsang, Gyorgy; Rozsondai, Bela *Magy. Kem. Foly.* **1970**, *76*, 236–240.
(5) Golberg, Michael A. *Solution Methods for Integral Equations: Theory and Application*; Golberg, Michael A., Ed.; Plenum Press: New York, 1976; Chapter 1.
(6) IMSL *MATH/LIBRARY, FORTRAN Subroutines for Mathematical Applications*; IMSL: Houston, TX, 1987.
(7) Adams, Ralph N. *Electrochemistry of Solid Electrodes*; Marcel Dekker: New York, 1969; Chapter 8.

* Author to whom correspondence should be addressed.

John W. Weidner
Peter S. Fedkiw*

Department of Chemical Engineering
North Carolina State University
Raleigh, North Carolina 27695-7905

RECEIVED for review October 31, 1989. Accepted January 29, 1990. This work was supported by a grant from the NASA-Lewis Research Center (NAG 3-649).